

Article

Radiant Floors versus Radiant Walls Using Ceramic Thermal Panels in Mediterranean Dwellings: Annual Energy Demand and Cost-Effective Analysis

Víctor Echarri-Iribarren ^{1,*}, Nyuk Hien Wong ² and Ana Sánchez-Ostiz ³¹ Department of Building Construction, University of Alicante, 03690 San Vicente del Raspeig, Spain² Department of Building, National University of Singapore, Singapore 119077, Singapore; bdgwnh@nus.edu.sg³ Department of Construction, Installations and Structures, University of Navarre, 31009 Pamplona, Spain; aostiz@unav.es

* Correspondence: Victor.Echarri@ua.es; Tel.: +34-965-903677

Abstract: The present study focuses on the application of large-format thermal ceramic conditioning panels (TCPs) containing polypropylene (PPR) capillary tube mats in dwellings on the Mediterranean coast. The thermal and energy behaviours were examined once the underfloor heating was installed, and they were compared with an alternative wall application. The system was implemented in a single-family house located on the Spanish Mediterranean coast. After having monitored the house during a complete one-year cycle, the annual energy demand was quantified using the Design Builder tool. TCP panels applied to radiant floors reduced energy demand by 5.15% compared to the wall-layout alternative. Significant reductions in CO₂ emissions were also achieved, as well as a 25.19% reduction in energy demand compared to convection systems. The incorporation of 24 m² of solar thermal panels into the system, combined with solar cooling systems based on lithium chloride, was also analysed. A reduction in energy demand of 57.46% was obtained compared to all-air convection systems. Finally, the amortisation periods of the investments in TCP panels and solar panels were calculated and compared to a convection system. Underfloor TCP panels proved to be more cost-effective than a wall installation. The additional cost of EUR 21,844 could be amortised over approximately 14 years with the radiant underfloor TCP system, while the wall TCP would be amortised over 17.4 years.

Keywords: integration energy and architecture; thermal ceramic panel; capillary tube mats; solar thermal panels; energy saving; renewable energy; investment amortisation



Citation: Echarri-Iribarren, V.; Wong, N.H.; Sánchez-Ostiz, A. Radiant Floors versus Radiant Walls Using Ceramic Thermal Panels in Mediterranean Dwellings: Annual Energy Demand and Cost-Effective Analysis. *Sustainability* **2021**, *13*, 588. <https://doi.org/10.3390/su13020588>

Received: 12 November 2020

Accepted: 6 January 2021

Published: 9 January 2021

Publisher's Note: MDPI stays neutral with regard to jurisdictional claims in published maps and institutional affiliations.



Copyright: © 2021 by the authors. Licensee MDPI, Basel, Switzerland. This article is an open access article distributed under the terms and conditions of the Creative Commons Attribution (CC BY) license (<https://creativecommons.org/licenses/by/4.0/>).

1. Introduction

Conditioning systems using radiant surfaces—floors, ceilings, or walls—provide high standards of comfort and can lead to significant energy savings. They have been used since ancient times, mainly underfloor, through hot air distribution. Today's solutions consist of various systems of production and distribution of air, water through thermoplastic tubes, copper wires, or radiant panels. Radiant heating systems are different from usual HVAC systems [1] because they heat or cool surfaces instead of propelling treated primary air to counteract internal and external thermal loads [2]. In addition, as pointed out by Feng et al., the size of the cooling loads varies substantially between both systems [3]. Underfloor systems based on hot water circulation through thick tubes, usually made of crosslinked polyethylene, have proliferated in recent decades because of the high standards of user comfort they offer [4]. Furthermore, this solution saves energy and allows incorporating alternative energies into the system, such as solar energy from solar thermal panels, or geothermal systems [5,6]. When distributing cold water from a chiller—a heat pump or a LiCl lithium chloride solar cold system—healthy cooling is achieved [7]. In humid climates, an additional dehumidification system is required.

A number of recent research projects have been conducted with hydronic radiant systems, in order to quantify hygrothermal comfort improvements [8,9] and the energy savings entailed by radiant systems [10]. Following a rigorous study, Lin et al. concluded that underfloor heating systems provide greater comfort while presenting a lower risk of airflows and reducing local user discomfort [11]. Mustakallio et al. compared chilled beam systems, chilled beam systems combined with radiant panels, and chilled ceiling installed mixing ventilation. They concluded that radiant systems also provide substantial energy saving and user-perceived comfort improvements [12]. Krzaczek et al. proposed an interesting pipe-embedded wall heating/cooling system in residential buildings which extracts heat from external enclosures and incorporates pipes through which water circulates [13]. Catalina et al. carried out an interesting study of radiant ceiling panels, concluding that they present higher comfort levels and consume less energy [14]. Sun et al. designed a flat heat pipe encapsulated within an aluminium panel used as a radiant surface, providing high thermal response speed and good thermal uniformity, together with low energy consumption [15].

When radiant system surfaces operate under humid climates, it is usually necessary to add a fan coil dehumidification system [16], or other efficient systems. Not only do such systems clearly improve user comfort, they also avoid moisture from condensing on cold surfaces. The challenge then becomes that of reducing energy consumption and limiting the costs of installation [17]. Sun et al. explored the possibility of coupling outdoor air cooling with underfloor cooling under a warm and humid climate, such as that of Korea; they achieved cooling energy savings of over 20% compared to usual cooling systems [18]. Fernández Hernández et al. proposed a prototype of hydronic underfloor heating integrating radiant floor cooling and an underfloor air distribution system (UFAD). The floor's cooling capacity increased, while the risk of floor surface condensation was averted [19]. Latest studies focus on combinations of these systems with phase change materials (PCMs) [20], which provide significant energy savings and reduce CO₂ emissions [21,22].

1.1. Radiant Surface Conditioning Systems Based on Capillary Tube Mats

The mid-1980s saw the development of radiant surface conditioning systems that were an alternative to thick tube systems: systems of mats of capillary tubes made of polypropylene (PPR). They are made with return manifolds of 20 mm in diameter, from which PPR tubes of about 3 mm diameter are laid out, approximately 10 mm apart [23]. Hot or cold water circulates through these mats, thus conditioning the buildings both in winter and summer. An added fan coil dehumidification system is required in summer. These mats can be applied to any surface indoors—floors, walls, ceilings—through various plasterboard, false ceilings, false walls or gypsum projection techniques and they procure healthy, quiet, and comfortable air conditioning. These systems function mainly by radiation, and secondarily by convection [24], as indicated by authors, such as Zhou and He, in their studies on surface temperature distribution [25]. Sound levels drop dramatically, because only low flows of indoor air are moved to dehumidify through low-power fan coils. When applied to cold floors, the impact of direct solar radiation significantly increases the actual cooling capacity, i.e., up to 1.44 times more than with the ISO 11855 method [26], as shown by Tang et al. [27] and Feng et al. [28]. This leads to a much greater level of user comfort [29], and save substantial amounts of energy [30]. Zhao et al. show that by incorporating solar energy via solar panels, the underfloor heating system can save significant amounts of energy and the investments made can be amortised over a short period of time [31]. Satisfactory results are being obtained from the application of chemical energy accumulation systems using solar thermal panels, functioning with lithium chloride: their future is promising [32,33]. The same applies to absorption systems based on solar thermal panels and geothermal energy systems [34] in which the mats act as ground exchangers at shallow depth [35]. Other studies propose applications on landscaped roofs [36] or using seawater [37,38].

Radiant systems using hot or cold water distribution have also been designed using prefabricated panels incorporating capillary tube mats. The most widespread finishing materials consist of laminated plaster, plasterboard, aluminium, steel sheets as shown in studies conducted by Tian et al. [39], and concrete [40], linoleum or high-density wood boards. Smoothed concrete solutions have also been developed for flooring. Mikeska et al. developed radiant concrete panels that incorporate capillary tube mats: they are proving to be a remarkable solution for high-occupancy areas because they eliminate the most sensible loads and significantly reduce ventilation airflow requirements [41]. Choi et al. proposed a vertical radiant panel for hospital room heating which have an impact on convection currents; they thus demonstrate the panels' best location for human health and to remove unpleasant odours [42]. Ručevskis et al. proposed panels or storage units containing capillary mats with PCMs, which accumulate energy by means of a night cooling system through natural air currents. The system is capable of absorbing daily thermal loads inside the room [43]. Ning et al. experimented with panels containing a thin layer of air, obtaining high efficiency when applying cooler water [44].

1.2. Description of TCP Ceramic Thermal Panels

In recent years, major technical improvements have been made to ceramic materials regarding mechanical strength and extremely low water absorption, especially with the technological development of porcelain stoneware, regarding both compression and extrusion manufacturing. The recent production of large format and low thickness panels makes them very light and easy to assemble. Pieces measuring up to 320 cm × 160 cm and 3 to 9 mm thick are obtained.

To solve the problem of uncomfotability due to its high effusivity and thermal conductivity values, multilayer solutions have been proposed, applied on site or using prefabricated panels, capable of offering more comfortable ceramic materials. For example, joule underfloor heating solutions with copper wire sheets have been patented [45]. Koschenz and Lehmann developed an interesting multilayer roofing system, incorporating capillary tube mats and PCMs, with a possible ceramic finish [46]. However, no application solutions had been combined to achieve capillary mat conditioning systems, using new large-format and low-thickness porcelain stoneware on floors, walls or ceilings [47].

One of the most recent initiatives has come from the research group "Technology and Sustainability in Architecture", of the University of Alicante. Together with Spanish Ceramic Tile Manufacturer's Association (ASCER) and the Institute of Ceramic Technology (ITC), the group developed and patented a large-format thermal ceramic conditioning panel (TCP) in 2010 [48]. It consists of: one or two pieces of large-format and low-thickness porcelain stoneware with fiberglass on one side; a capillary mat of PPR polypropylene tubes 3.5 mm in diameter and 10 mm apart; and conductive paste to adhere the capillary tube mat and ensure good thermal conductivity from the capillary mats to the ceramic (Figure 1a). The panel could also be made with two ceramic pieces on each face, ensuring the emission of energy by radiation on both surfaces. It thus allows it, for example, to be hanged vertically from the ceiling in a baffle-like solution. The solution is ideal for flooring, floating floors, false modular ceramic ceilings, large-format pieces of wall or ceiling plasterboard, as well as ceiling coverings generally.

Prototypes of TCP panels were recently made and installed on two adjacent walls, in two offices belonging to two different buildings of the University of Alicante. In one of them, which operates with an all-water air conditioning installation, a specific circuit has been channelled to serve a small 12 m² office and a management substation was installed. The existing connections to the fan coil have been directed towards the distribution to four radiant panels measuring 2.5 × 1 m. (Figure 1b). Home automation was applied to the installation and the system can be controlled remotely. Modbus EIM3155 63A electric consumption meters and Modbus MULTICAL 602 KAMSTRUP hot or cold water energy meters for a nominal flow rate of Q_n 0.6 m³/h (Figure 1c) were set up.

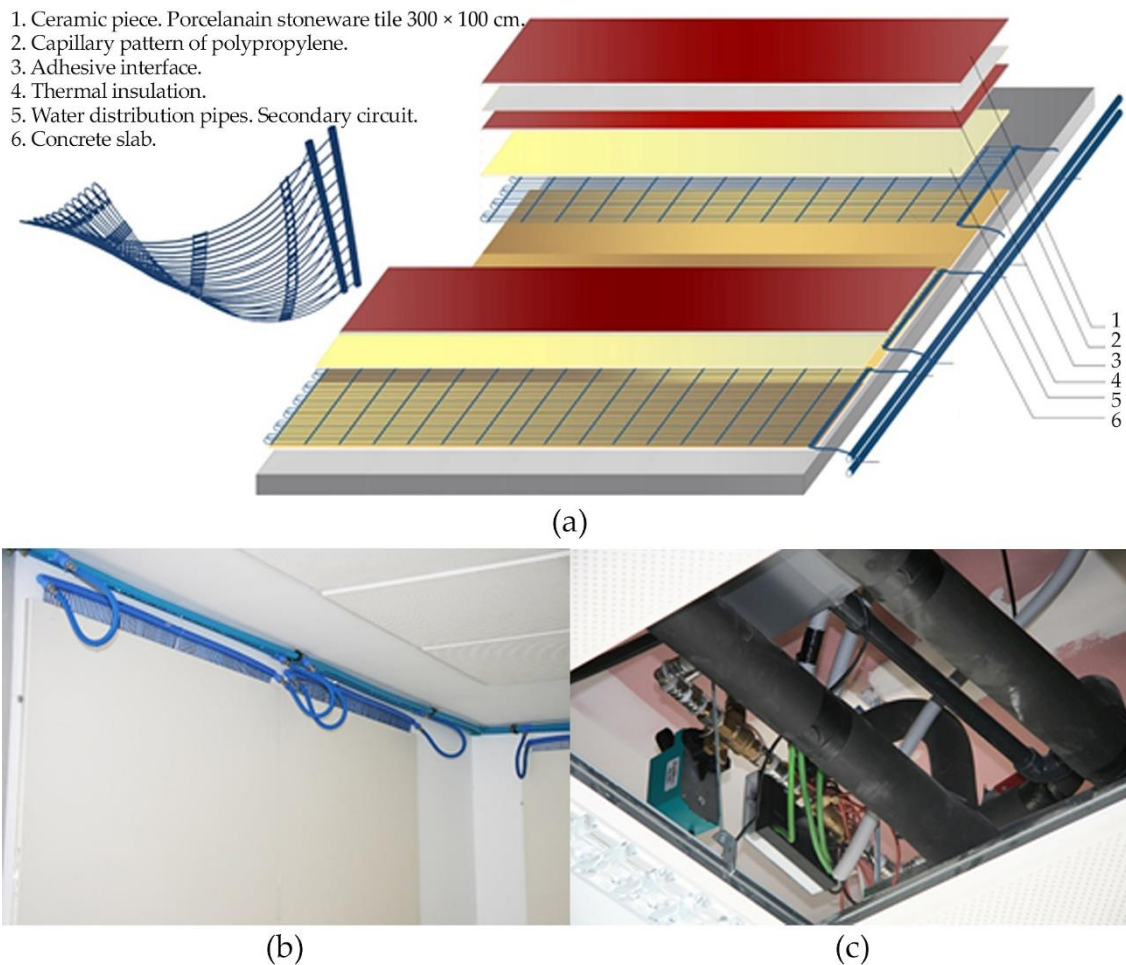


Figure 1. (a) Large-format thermal ceramic conditioning panel (TCP) placed on the floor. Patent application no. P201001626; (b) installation of the TCP in an office at the University of Alicante; (c) Energy meter for Q_n 0.6 m³/h of hot/cold water. Modbus MULTICAL 602 KAMSTRUP.

1.3. Objectives

This study describes the implementation of large format thermal ceramic conditioning panels (TCP) in an isolated detached house located at the crossroads of Calle Horacio and Calle Virgilio in Alicante (Calle Virgilio n° 6, 38°22′03.2″ N 0°26′33.5″ W), 500 m north of the Albufereta beach (Alicante, Spain). Previous research presented the results after applying TCP panels on some walls [49] across various combination scenarios, including a bioclimatic basement environmental tempering technique. For the present work, the TCP panels were applied as an underfloor heating system, following the experience gained at the Museum of the University of Alicante [7]. It would be possible to condition the house in winter and summer, using dehumidification system based on three fan coils. The annual energy demand and the CO₂ emissions deriving from the use stage of these two TCP panel placement systems—underfloor and wall—were compared both among themselves, and to conventional convection systems. This is the key research issue of this study, whose novelty consists of the application of TCP panels, containing capillary tube mats, on underfloor heating in detached houses on the Mediterranean coast, and its comparison with the application on walls. It has never been done before, and its contribution to the current academia can be relevant for the energy savings and CO₂ emissions derived. The option of incorporating a solar thermal panel system on the flat roof was also discussed. It would be applied to the hot water production system in winter, and water cooling through chemical energy (solar cold), providing alternative energy to the system. As we will see, significant

energy savings can be achieved, with adequate amortisation periods of the investments required. We also sought to test the hypothesis that the amortisation period of underfloor TCP panels would be shorter than that of wall TCP panels.

The area around Albufereta beach in Alicante is under a Mediterranean climate. It receives high levels of solar radiation on most summer and winter days, reaching an average value in August of 380 W/m^2 during daylight, and can exceed 600 W/m^2 at certain times during the month. According to the classification of Köpen-Geiger [50], it corresponds to BSh: a warm semi-arid climate with hot or very hot summers, and mild winters with little rainfall [51]. During the months of September and October, the cold drop (*gota fría*) phenomena can occur, i.e., abundant rainfall at specific times.

2. TCP Panels Used as Underfloor Heating in a Detached House

The detached house under study consists of prism-shape volumes finished in single-layer white mortar (Figure 2). It includes a basement, a ground floor and a first floor, with a total constructed area of 346 m^2 . A $4.2 \times 4.2 \text{ m}$ side patio runs vertically along the three floors, from the basement to the first floor. Most of the glazing has been installed in this courtyard and in two other smaller courtyards located on the ground floor (Figure 2). This way, the house barely receives thermal loads from solar gains in summer.

Initially, the house was designed with a ground floor and first floor only. Given the ground's low resistance, however, a basement was finally built covering the whole of the floor's surface area. The moderate temperatures of the basement's reinforced concrete walls were used to mitigate the indoor air as well as the surface temperatures of the walls of the rest of the house. A passive conditioning system was generated by convection currents, leading to a drop in energy demands and increased hygrothermal comfort (Figure 2e). This passive system could be combined in summer with the opening of the living room's large glass panes on the ground floor, the kitchen patio panes and the bedroom ones on the first floor, generating convection currents depending on the outdoor air conditions. An all-air system with a heat pump was designed for summer and winter conditioning. To obtain satisfactory thermal conditioning in winter, a heating system with hot water radiators was also installed.

Deficiencies in construction quality and low-standard regulatory requirements proper to southeastern Spain (NBE-CT-79) were thus compensated. In the region, VRV split-type air conditioning facilities proliferated in homes, usually years after they were built. Facades are filled with poorly integrated condensing machines. The latter reflects the failures of a construction policy that has overlooked passive conditioning techniques. Compared to standards, such as Passivhaus, with energy demands below $15 \text{ kWh/m}^2\text{yr}$ in winter, southeastern Spain usually presents ranges between 25 and $50 \text{ kWh/m}^2\text{yr}$ in winter, and much higher values in summer [52,53]. The energy demand of buildings would be excessively high if the indoor air's temperature and relative humidity conditions were not usually set below the recommended standards. Many people resort to having a second home in different climatic zones to cope with summer and meet the conditions for their personal health.



Figure 2. Description and distribution of the detached house. (a) View of the house on its northeast facade. Outdoor porch of the living room and pool; (b) basement; (c) ground floor; (d) first floor; (e) longitudinal section through the courtyard. The basement acts as a passive bioclimatic system.

2.1. Constructive Solutions of the Project at Its First Stage

The building's enclosures were designed in accordance with the requirements of Spanish regulations (CTE in its Spanish acronym). Table 1 shows the different materials that make up the building's walls, floor and roof.

Table 1. Material layers and U -value of different enclosures of the project.

		U W/m ² °C	Material	Espesor (cm)
E1	Enclosure	0.435	Single-layer mortar	1.5
			Double hollow brickwork	12
			Rock wool insulation	5
			Air chamber	4
			Single hollow brickwork	7
			Double plasterboard on steel substructure	3 + 3
E2	Enclosure	0.462	Single-layer mortar	1.5
			Concrete block	20
			Rock wool insulation	5
			Double plasterboard on steel substructure	3 + 3
W	Windows	3.10	Large double-glazed sliding windows on anodised aluminium frames, with thermal break	4
F	Floor	0.482	Reinforced concrete foundation slab	60
			"Cupolex" plastic pieces to create a camera	60
			Waffle slab with reinforced concrete ribs	15
			Thermal insulator. Type IV expanded polystyrene	4
			Regulatory layer. Self-levelling cement mortar	10
			Wooden strips for laying the floor	4
			Canadian oak flooring	2
R	Roof	0.403	Gravel diameter 20 mm	5
			Protective Geotextile	0.4
			Thermal insulation of extruded polystyrene	6
			LBM-40 waterproofing bituminous film	0.3
			Formation of cellular concrete slopes	10
			Reinforced concrete ribbed waffle slab	27
			Plasterboard on steel substructure	1.5 + 3

2.2. Installation of TCP Panels as a Conditioning System

During the project phase, we decided to use PPR capillary tube mats in the ceiling, covering a total surface of 235 m². A 40 kW heat pump project was drafted, including a substation with a heat exchanger and secondary circuit. In the second phase of the project, we studied the application of TCP panels to the radiant floor. A total area of 260 m² was laid out, larger than the ceiling area (235 m²) and below what would be required if the basement's passive conditioning was not available in summer. The installation of thermal solar panels on the roof was also contemplated, through a solar cold system using lithium chloride chemical energy [32]. The technical characteristics of the conditioning system are shown in Table 2.

Table 2. Technical characteristics of the capillary tube mats and solar energy system.

Units	System Components	Diameter	Power	COP	EER
1	Air-water heat pump with two inverter scroll compressors (refrigerant R410A)		40 kW	4.11	2.85
10	Flow circuits of PPR tubes with thermostatic valves	20 mm			
10	Return circuits of PPR tubes with balancing valves	20 mm			
3	Fan coil dehumidifiers		0.5 kW		
24 m ²	Thermal solar panels for a solar cold system LiCl		27 kW		

The new constructive solution adopted is shown in Figure 3. The system complies with the sound insulation established in the CTE; it also presents high mechanical resistance. The system is fully recordable in the skirting boards via small aluminium doors throughout the perimeter, thanks to the width of all spaces being below 6 m. The floors are thus designed using two TCP pieces and manifolds on both walls (Figure 4).

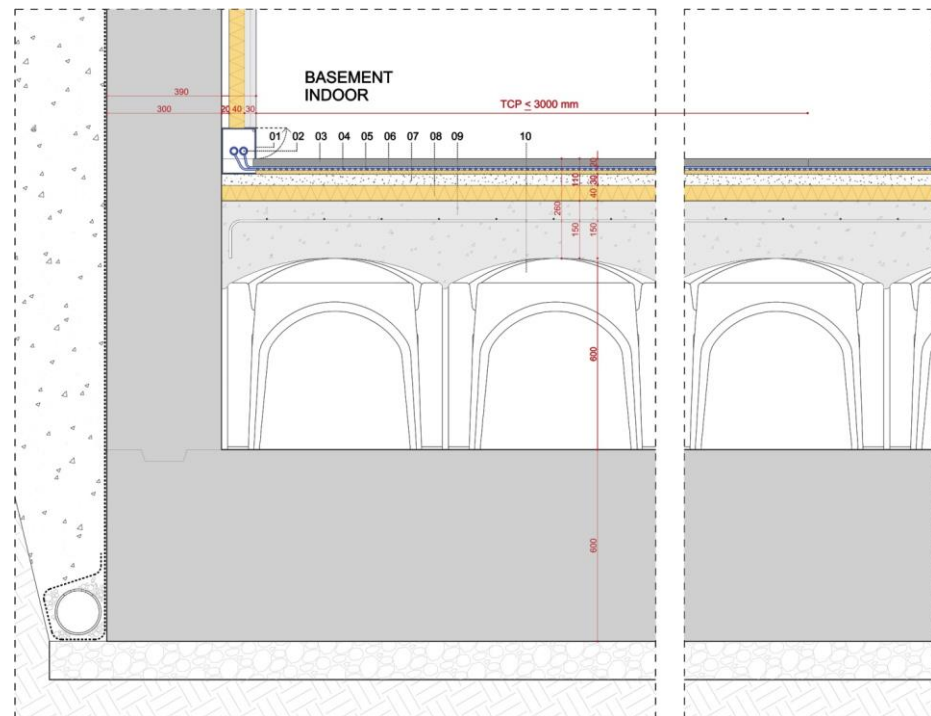


Figure 3. Thermal ceramic conditioning panel applied to the house floor.



Figure 4. Possible on-site application of the TCP panels in its different layers.

1. PPR distribution pipes. Diameter: 32 mm.
2. Aluminium channels to pass the PPR distribution pipes through.
3. Large-format porcelain stoneware piece. $300 \times 100 \times 2$ cm.
4. Adhesive layer. Beka Thermal Conductive Paste V. WLP. 1. Thickness: 6 mm.
5. PPR capillary mat. Diameter: 3 mm. Separation: 10 mm.
6. Polyurethane foam thermal insulator. Thickness: 10 mm.

7. Regulatory layer. Self-levelling cement mortar. Average thickness: 10 mm.
8. Thermal insulator. Type IV expanded polystyrene. Thickness: 40 mm.
9. Waffle slab with reinforced concrete ribs. Thickness: 270 mm.
10. "Cupolex" plastic pieces to increase and create a camera on the reinforced concrete slab foundation.

3. Methodology

To achieve the objectives of the research, the house was monitored during the whole 2012 cycle, retrieving data on the thermal behaviour of the interior surfaces, indoor and outdoor air speed, indoor and outdoor air relative humidity and temperature, and solar radiation. Air infiltration through the enclosure was measured using the Blower Door test [54]. Thermal bridges were also evaluated with the AnTherm tool (Vienna, Austria). The bioclimatic effect of the basement was reflected in the wall surface temperatures and in the indoor air temperature and relative humidity (RH).

Subsequently, working scenarios were defined to compare the thermal behaviour, energy demand and derived CO₂ emissions. The following scenarios combined different options regarding the air conditioning system, the use of the basement in the conditioning, and the installation of thermal solar panels on the roof (Table 3):

1. Scenario 1 (SC1). Current status. Bioclimatic basement supporting the conditioning of the house. All-air system. Heating-based support system through hot water radiators and a cold air system in summer with a compression system on the roof and an evaporator in the bathroom.
2. Scenario 2 (SC2). Bioclimatic basement supporting the conditioning of the house. Application of TCP panels to walls. Dehumidification in summer through three fan coils, one on each floor.
3. Scenario 3 (SC3). Bioclimatic basement supporting the conditioning of the house. Application of TCP panels to radiant floor. Dehumidification in summer through three fan coils, one on each floor.
4. Scenario 4 (SC4). SC3 conditions but with thermal solar panels on the roof.

Table 3. Working scenarios of this research.

Scenario	Conditioning System	Use of the Basement	Thermal Solar Panels
SC1	All-air system in summer with radiators in winter	Bioclimatic basement	
SC2	TCP panels as radiant walls	Bioclimatic basement	
SC3	TCP panels as radiant floor	Bioclimatic basement	
SC4	TCP panels as radiant floor	Bioclimatic basement	Solar cold system LiCl

To compare the energy demand and CO₂ emissions derived from the different scenarios, the four scenarios were adjusted to an operating temperature T_o , and a similar relative humidity (RH) range between 45% and 55% was established in all of them, which guarantees a similar level of comfort for users. T_o can be defined as "the uniform temperature of an imaginary enclosure in which the body exchanges the same dry heat for radiation and convection as in the same real environment, regardless of latent loads" [55]. The user's sense of comfort will depend on various factors, such as the exchange of heat by convection and radiation with the indoor air and the surfaces of the environment respectively, the capacity to emit water vapour into the indoor air by perspiration and breathing, as well as the quality of the indoor air.

3.1. Calculating the Operating Temperatures T_o

The parameters that directly determine sense of comfort were analysed, mainly: the dry air temperature, its relative humidity, the speed of the surrounding air, and the surface temperature of each of the wall surfaces making up the room [55]. To work with similar

user comfort levels in this study, in addition to the operating temperature T_o , the values of heat loss by radiation and convection were quantified and unified. The usual values of user sensitive heat emission are around 105 W. Heat losses from convection and radiation (q_{rdi} and q_{cvi}) were obtained through the Expressions (1) and (2):

$$q_{cvi} = h_c(T_i - T_a) \quad (\text{W/m}^2) \quad (1)$$

$$q_{rdi} = h_r(T_i - T_{rm}) \quad (\text{W/m}^2) \quad (2)$$

The convection factor h_c is directly related to air velocity. It usually has an average value of $3.5 \text{ W/m}^2 \text{ }^\circ\text{C}$, with an air speed of 0.1 m/s . The air speed was set to 5 cm per second for TCP panels, obtained on site in the monitored offices, and 15 cm/s in the all-air installation, as the average value of the area of occupancy obtained on site. Values of factor h_c were obtained through Expression (3). The coefficient of loss by radiation h_r had approximate values of $4.7 \text{ W/m}^2 \text{ }^\circ\text{C}$ with an estimated human body temperature T_i of $30 \text{ }^\circ\text{C}$.

$$h_c = 14.11 \times v^{0.24} \quad (\text{W/}^\circ\text{C}) \quad (3)$$

The values of operating comfort temperature T_o were calculated according to the Expression (4), with values of mean radiant temperature T_{rm} according to the Expression (5):

$$T_o = \frac{h_r T_{rm} + h_c T_a}{h_r + h_c} \quad (4)$$

$$T_{rm} = T_1 \times F_{P-1} + T_2 \times F_{P-2} + \dots + T_N \times F_{P-N} \quad (5)$$

3.2. Thermal Loads

The sensible and latent thermal loads were mainly calculated using the Design Builder tool (Stroud, UK). Some of them, such as the U -value of the enclosures and the loads due to air infiltration, were carefully calculated with some previous data taken on site.

3.2.1. U-Values: Thermal Transmittance of the Enclosures

Fourier's law, which applies to parallel layers of materials, of an unlimited surface, in steady state indoor T_i and exterior T_e air temperatures, establishes the temperature gradient reached by multi-layer enclosures when there is a thermal gap between outdoor and indoor air temperatures (Equation (6)).

$$U - \text{value} = \frac{1}{R_T} = \frac{1}{\frac{1}{h_i} + \sum_0^n \frac{e_i}{\lambda_i} + \frac{1}{h_e}} \quad (6)$$

where:

R_T Total thermal resistance to the passage of heat.

$1/h_i$ Interior surface thermal resistance.

$1/h_e$ External surface thermal resistance.

e Thickness of each layer.

λ Each layer material's thermal conductivity.

The usual values of thermal conductivity λ of the materials used in the enclosure, according to UNE-EN-ISO 10456: 2012 [56]. The thermal inertia of the materials making up the enclosure alters the linear Fourier process as a function of time, since the thermal gap between exterior and interior air temperature, the solar radiation that affects the exterior surface, or the interior air conditioning systems vary according to the weather. Heat flow thus becomes a dynamic and complex process, which can be solved by specific tools as Design Builder.

To perform building behaviour simulations in terms of energy demand and interior comfort parameters, and to quantify the energetic impact, the transmittance U -values of all the enclosures obtained through Equation (6) were introduced into the Design Builder tool.

3.2.2. Air Infiltration through the Envelope

The air infiltration value through the enclosure was forecast to be very low thanks to the construction's quality, the seals used, and the joinery quality. It was evaluated by means of the Blower Door test conducted in accordance with the European Standard EN 13829, using the BlowerDoor GMBH MessSysteme für Luftdichtheit equipment. The impact of annual energy demand due to air infiltration was evaluated using a simplified model (Equation (7)), applying the concept of degree-day, which relates the average temperature outside the house under study and the interior comfort temperature (21 °C for heating and 24 °C for cooling).

$$Q_{inf} = C_p \times G_t \times V_{inf} \quad (7)$$

where:

Q_{inf} Annual energy loss (kWh/yr) due to air infiltration for heating Q_{inf-H} and cooling Q_{inf-C} .

C_p Air's specific heat capacity, which is 0.34 Wh/m³K.

G_t Annual degrees-days (kWh/yr), both for heating and cooling.

V_{inf} Air leakage rate (m³/h).

Sensible and latent heats were quantified by means of the following Equations (8) and (9):

$$Q_s = V_{inf} \times C_e \times \rho \times (T_e - T_i) \quad (8)$$

where:

Q_s Energy impact value of the sensible heat of the air leak rate V_{inf} (W).

V_{inf} Air leakage rate (m³/h).

C_e Specific heat of the air under normal conditions 0.349 Wh/kgK.

ρ Density of air (kg/m³).

T_e Outside air temperature in degrees Kelvin (K).

T_i Air temperature inside the house (21 °C in winter and 24 °C in summer).

$$Q_l = V_{inf} \times C_v \times \rho \times (W_e - W_i) \quad (9)$$

where:

Q_l Energetic impact value of the latent heat of the air leak rate V_{inf} (W).

C_v Heat of water vaporization (0.628 W/g_{vapour}).

W_e Specific humidity of the external air taken as the annual average value (g_{vapour}/kg).

W_i Specific humidity of the indoor air (g_{vapour}/kg).

3.3. Simulations of Thermal Behaviour: Annual Energy Demand

Energy behaviour simulations and energy demand calculations were performed in the Design Builder tool for the four scenarios SC1–SC4. The following parameters were set:

1. The winter period covers 1 December to 30 April, and the summer period 1 May to 30 November. These are the usual weather conditions in Alicante.
2. Indoor air set temperatures were 21 °C in winter and 24 °C in summer. Relative humidity (RH) remained at 50%.
3. Occupancy, according to the CTE's regulatory calculation for air renewal, is six people. Since the interior volume is 302 m³, the requirement for forced air renewal is 0.32 air changes per hour (ACH), equivalent to 12 L per second per person.
4. Air infiltration through the enclosure was measured using the Blower Door test. The result was 0.342 ACH, a low value for a detached house [57], far from the Passivhaus standard (<0.6 ACH).

5. We estimated load gains or losses due to thermal bridges at 3.5% of total thermal loads [58] by thermal transmittance U of the enclosures [59,60].

The schematic diagram of the capillary tube mats project was introduced into the Design Builder model (Figure 5). The surface temperatures of the TCP panels were then pre-set to 17 °C, to avoid the risk of surface condensations. We also introduced the climate file relating to external air temperatures, relative humidity, and solar radiation levels by pyranometer throughout a complete one-year cycle. The dehumidification of the three fan coils was also applied, with a total power of 1500 W.

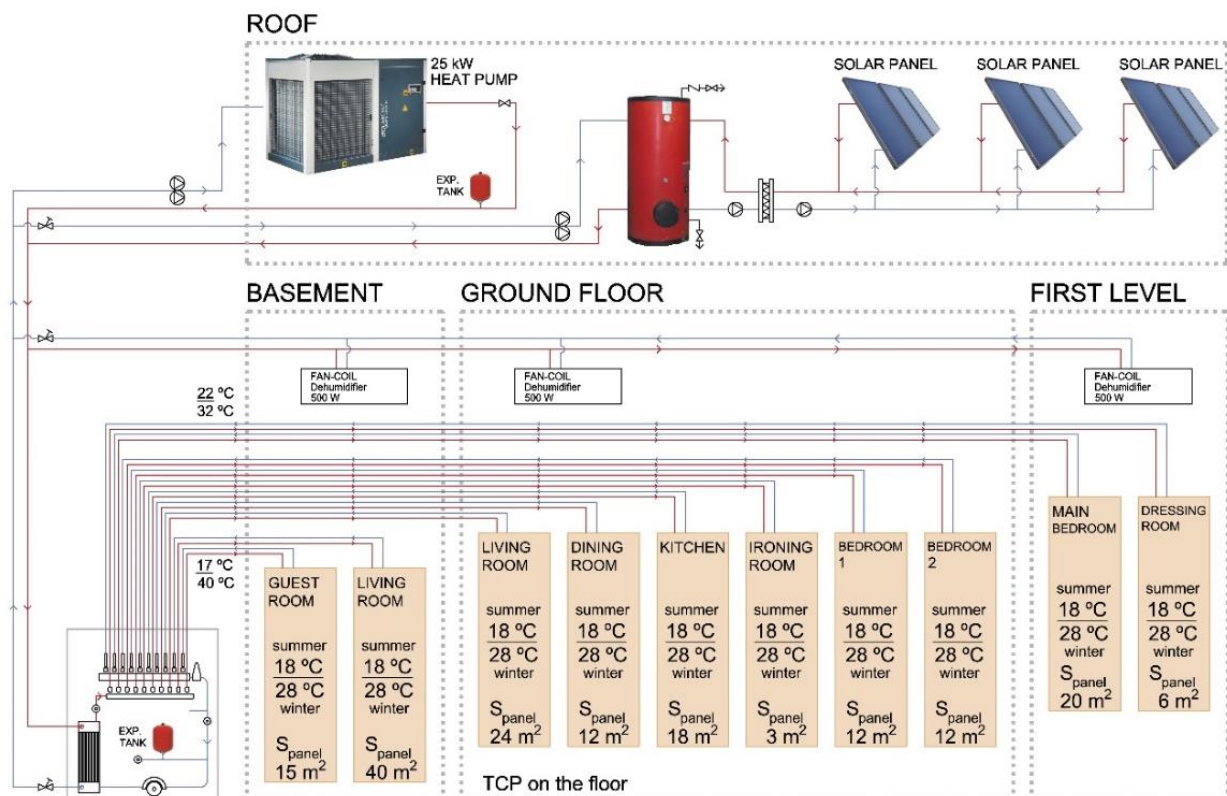


Figure 5. Schematic diagram of the installation of capillary mats and fan coil dehumidification. Later modelled in Design Builder.

To calibrate the model and adjust it to the actual thermal behaviour, the climate file obtained in situ was used. It was modified until it was adjusted to the air infiltration value through the envelopes, varying the values in the Design Builder simulation tool. The annual energy demand obtained was thus adjusted to the real energy consumption obtained from the meters. The average energy consumption for the period 2012–2014 was 20,559.6 kWh/yr. Once the value of lighting and household appliance consumption was subtracted, which was 4.8 kWh/m²yr, the annual energy consumption value of 19,110 kWh/yr for radiator heating and existing summer conditioning was obtained.

3.4. Energy Contribution of Solar Thermal Panels

As previously mentioned, the TCP system distributes hot and cold water at moderate temperatures, making it easier to incorporate alternative energies such as solar energy. Following the comparative analysis of the SC1–SC3 scenarios regarding the energy savings generated by implementing TCP panels as a radiant floor, combined with the bioclimatic basement, the application of solar thermal panels on the roof (SC4) was simulated in order to evaluate the energy savings and the investments' amortisation period. These solar thermal panels operate by heating the system's water in winter or cooling it in summer by means of an absorption cooling system based on lithium bromide LiBr [61], or LiCl

chemical energy (solar cold) [62,63]. The solar radiation power data on the roof of the detached home was collected for the whole 2012 cycle, through a pyranometer (KIPP Model CMP3 pyranometer ISO second class). The results obtained in August varied between 150 and 600 W/m² and those obtained in February between 100 and 300 W/m². These values bear similarities with the results reported in other recent studies—e.g., the Museum of the University of Alicante [7]—sources and publications, which include these values for the Mediterranean and southeast Spain [64]. The performance of an installation of solar thermal panels, at a 38° latitude of location and 45° inclination, can be obtained from other previous studies [65], as well as the overall performance of the installation [66].

3.5. Investment Amortisation Approach

The last section of this comparative analysis focuses on the feasibility of implementing the TCP panel system and combining it with solar thermal panels in the real estate market. These technical installations based on capillary tube mats could be introduced into the same type of single-family homes as those in the Albufereta area. We thus estimated the system's return on investments over a building's life cycle. To make this estimation, we applied the methodology used in previous studies [7], which could serve as a reference for other buildings on the Spanish Mediterranean coast. The tool used is the Life Cycle Cost (LCC), which was applied in accordance with the standard UNE-EN 15459-1:2017 [67]. The protocol was followed for the four scenarios—SC1, SC2, SC3 and SC4—designed for this study. The most complex parameter to quantify was the Global Cost, which was obtained through the following expressions:

$$C_g(t) = C_l + \sum_j \left[\sum_{i=1}^t (C_{a,i}(j) \cdot R_{disc}(i)) - Val_{E,t}(j) \right] \quad (10)$$

$$R_R = \frac{R_{int} - R_i}{1 + R_i/100} \quad (11)$$

$$R_{disc}(i) = \left(\frac{1}{1 + R_R/100} \right)^i \quad (12)$$

where:

C_g Global cost.

C_l Initial investment costs including indirect cost too.

$C_{a,i}$ Annual costs including maintenance, energy and replacement costs.

R_{disc} Discount rate. Depends on the real interest rate (R_R) and the cost period considered (number of years from the initial year). Calculated according to expression 3

i years.

$Val_{E,t}$ Residual value of components at the end of the calculation period, considering depreciation of their initial investment.

R_R Real interest rate. Depends on the market interest rate (R) and the inflation rate (R_i), both may depend on year i , but here they will be considered constant.

R_i Inflation rate.

R_{int} Interest rate.

The investment costs of building the whole house, including installations and execution, indirect costs, costs due to periodic maintenance, and replacement costs, over a 30-year period as established by the UNE-EN 15459-1:2017, were obtained from various databases of companies in the sector in Alicante.

4. House Monitoring

The house was monitored in two stages. The first monitoring system consisted of sensors (wall temperature, indoor air temperature, outdoor air temperature, relative humidity (RH), air speed and solar radiation using a pyranometer on the roof) placed at strategic points of the enclosures. The data collected by the sensors were sent to a data

logger (analyser), which transmits the signal via General Packet Radio Service (GPRS) to a database (Figure 6). This information is accessible from a web platform. The GRD GSM/GPRS data logger allows data to be recorded via analogue or digital channels. Using its GSM/GPRS modem, data is sent to a server and can be consulted on the web in chart and table formats. They are downloaded as a comma-separated values (CSV) file. Data were collected for the whole 2012 cycle.



Figure 6. Analyser and sensors located on the wall.

In a second phase, monitoring was carried out using a wireless system. Temperature sensors were connected to small analysers, model “EL-WiFi-TC-Thermocouple Probe Data logger”. The analysers “EL-WiFi-TH, Temperature and humidity data logger”, with built-in temperature and relative humidity probes, interpret the recorded data and send WiFi signals to a laptop. By installing the software “EasyLog WiFi Software”, the data are received and stored on the computer. Through a custom code you can access the information from any computer over the network. This second monitoring operation was carried out during the week of 1 to 7 February 2012, and from 1 to 7 August 2012. Surface temperature, indoor air temperature, and RH data were taken elsewhere in the house allowing a faster and more adjusted calibration of the model in Design Builder.

Flyr’s ThermaCam P 25 thermal imaging camera was used to detect thermal bridges. U thermal transmittance and Ψ linear thermal transmittance values were obtained in joints, singular points and structural points [68]. They were quantified using the AnTherm software, and load gains or losses due to thermal bridges were estimated at 3.5% of total thermal loads due to thermal transmittance U of the enclosures [69], i.e., similar values to those obtained in previous studies [49].

5. Results

The application of TCP thermal ceramic panels on some of the house’s walls (SC2) had been simulated in previous studies and the results were published in 2017 [49]. The application of TCP panels together with the effect of the bioclimatic basement reduced

annual energy demand by 12%. Results of this parameter were obtained with set operating temperatures T_o of 20 °C in winter and 24 °C in summer, an occupancy of 1 person per 50 m², ventilation airflow of 0.63 ACH, and infiltration airflow of 0.342 ACH. The application of wall ceramic thermal panels was also compared to the all-air conditioning system in summer, and hot water radiators in winter. The results for user thermal comfort were equally satisfactory in summer and winter regimes, as the radiant system was capable of dissipating, by means of radiation and convection, around 60 W of heat per square metre of body surface in the summer regime [55].

5.1. Calculation of Operating Temperatures T_o

The indoor air temperature data T_i obtained through the monitoring were obtained with and without the air conditioning system turned on. The Design Builder tool was used to simulate indoor air temperature data for the SC3 with underfloor TCP panels with PPR capillary mats (Figure 7).

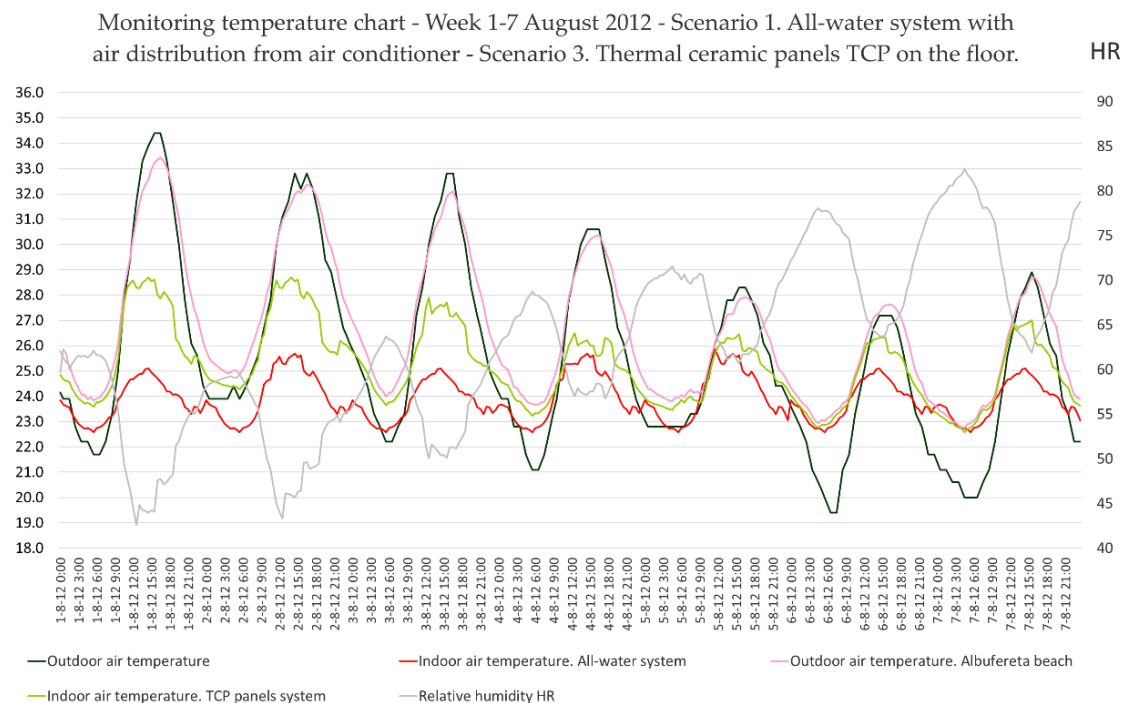


Figure 7. Outdoor and indoor air temperatures (T_i, T_e) and relative humidity (RH) in summer. All-air system (SC1), and TCP panels on the floor (SC3).

As can be observed in Table 4, the operating temperatures T_o for the living room on the ground floor are close to the values of 24 °C. In the case of the house under study, the indoor air temperature in summer from 1 to 3 August 2012 was between 2 and 3 °C higher with the radiant systems compared to the convective systems, and around 1.5 °C on 4–7 August.

Table 4. Calculation of operating temperatures T_o in summer for the 4 Scenarios.

	v	h_c	T_a	h_r	T_{rm}	T_o
	m/s	W/°C	°C	W/m ² °C	°C	°C
SC1	0.160	9.088	24.07	4.70	23.98	24.035
SC2	0.082	7.742	26.11	4.70	19.45	23.598
SC3–SC4	0.085	7.759	26.24	4.70	19.28	23.617

5.2. The Value of Annual Energy Demand

Spanish regulations on energy efficiency in buildings, i.e., the technical document DB-HE on energy saving, which is part of the Technical Building Code (or CTE by its Spanish acronym) makes it mandatory to apply the standardised tool Lider-Calener HULC [70] to architectural projects. The instrument, however, presents notable shortcomings compared to other simulation instruments, such as Design Builder or TRNSYS. For the present study, the Design Builder tool was chosen for its proven reliability with the EnergyPlus calculation engine (Figure 8).

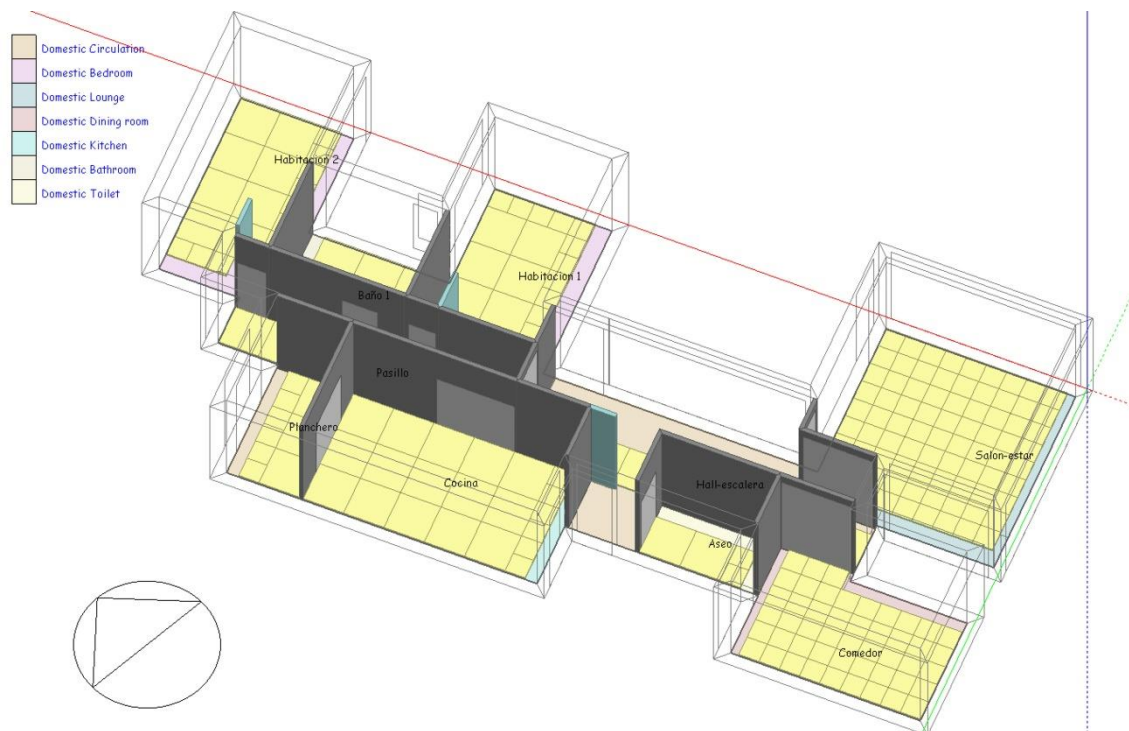


Figure 8. Location model of radiant floor TCP panels. Design Builder.

To perform the simulations of the house's thermal and energy behaviour, data on indoor set air temperature T_i , people occupancy, renewal air flow, infiltration air, etc. exposed in 3.2 were introduced in the Design Builder tool (Figure 9). The schematic diagram of the capillary tube mats project was introduced into the Design Builder model (Figure 5). Surface temperatures of TCP panels were then set at 17 °C, to avoid the risk of surface condensation. The climate file relating to external air temperatures, relative humidity, and solar radiation levels obtained by pyranometer throughout the full cycle of 2012 was also introduced [7,49]. Finally, the infiltration value was adjusted to 0.342 ACH, so that the model was calibrated by adjusting the indoor air and wall surface temperatures to the values obtained by monitoring. In a second phase, the actual energy consumption of 19,110 kWh/yr, obtained from the meter [49] were adjusted to the annual energy demand values. The three fan coils dehumidification system was introduced, with a total power of 1500 W.

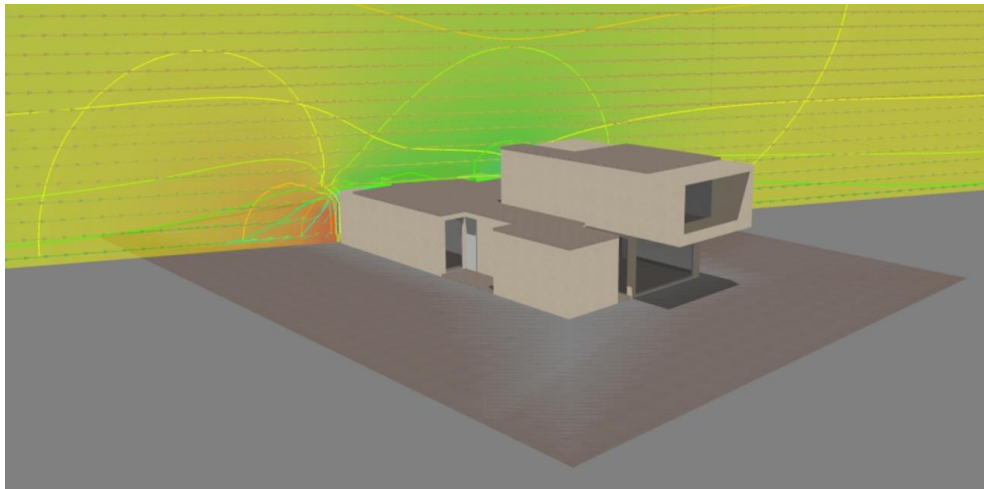


Figure 9. Model in Design Builder. Radiant system using TCP panels. Outdoor temperature gradients.

Table 5 lists the results of thermal loads and solar gains obtained during the simulation through Design Builder for the SC1 (VRV Split system and the currently installed hot water radiators) and SC3 (TCP panels) scenarios [3,71]. When using radiant TCP panel underfloor systems, these thermal loads would be reduced by 23.91% in summer and 27.56% in winter. The heat flows by U transmittance drops from 17.422 to 8.305 kWh/m²yr in summer, and from 30.758 to 25.250 kWh/m²yr in winter.

Table 5. Calculation of thermal loads and final energy demand in winter and summer.

	All-Air SC1		TCP Radiant Floor SC2	
	Summer Wh/m ² yr	Winter Wh/m ² yr	Summer Wh/m ² yr	Winter Wh/m ² yr
Enclosure				
Glazing	7568	11,379	4192	10,399
Walls	812	122	392	142
Floors—ground	−724	3610	−675	2233
Partitions	0	0	0	0
Rooftops	2539	4034	1179	2741
Outdoor floors	149	95	142	78
Infiltration	7078	12,230	3075	9657
	17,422	30,758	8305	25,250
Loads				
Lighting	1161	1606	1161	1606
Equipment	1811	1507	586	595
Occupation	4308	3955	4308	3955
Solar gains	18,538	−14,536	18,538	−14,536
	25,818	−7468	24,593	−8380
	kWh/m ² yr	kWh/m ² yr	kWh/m ² yr	kWh/m ² yr
Primary energy	43.24	23.29	32.90	16.87

Table 6 shows the results obtained by simulating summer, winter and annual energy demands over the four Scenarios SC1–SC4. While PPR capillary tube mat systems have been shown to produce energy savings ranging between 30 and 35% compared to convective systems in Central Europe [72], these savings were somewhat lower in the Albufereta house. The outdoor air RH is obviously higher on the Mediterranean coast than in Central European countries, and further dehumidification of indoor air is needed. Annual energy demand in the actual state (SC1) is 66.53 kWh/m²yr for the split system with an evaporator in the bathroom, distribution of treated air through pipes, and heating through hot water

radiators in winter. In the case of SC3, with the application of floor TCP panels, annual energy demand drops to 49.77 kWh/m²yr. The resulting energy savings amount to 25.19%. These reductions are greater than those obtained in previous studies [47] for SC2 where TCP panels were applied to the wall, which had amounted to 21.13%.

Table 6. Summer, winter, and annual energy demand over the four scenarios SC1–SC4.

	SC1	SC2 TCP Walls	SC3 TCP Floor	SC4 TCP + SOLAR
Energy demand in summer kWh/m ²	37.15	28.63	26.95	17.09
Energy demand in winter kWh/m ²	29.38	23.84	22.82	11.21
Annual energy demand kWh/m ² yr	66.53	52.47	49.77	28.30
Annual CO ₂ emissions in use stage	7835.10 kg	6179.28 kg	5861.13 kg	3332.73 kg
Percentage	100.00%	78.87%	74.81%	42.54%

Results shown in Table 6 allow us to conclude that the energy demand of the all-air system with air-to-air heat pump for air distribution in SC1 is 126.8% higher than water distribution to TCP panels in radiant walls in SC2, and 133.7% higher than in SC3 with underfloor TCP panels. If the TCP panels are installed as a radiant floor (SC3), the annual energy demand is reduced by 5.15% compared to the TCP solution on the wall (SC2). The radiant floor's convection currents produce a better temperature gradient in the indoor air and a slightly lower T_{rm} in summer and somewhat higher in winter, as well as a slightly higher T_a in summer and somewhat lower in winter, with a T_o similar to SC2. This brings about a reduction in heat losses by transmission through opaque and glass enclosures. Consumption due to dehumidification, with the two 1500 W fan coils in the TCP panels, is 1547 kWh/yr, a high value that would make these systems a priori less favourable in summer. However, the savings derived from the much lower amount of energy needed to transport water compared to air, as well as the thermal load drop thanks to the reduced thermal gap of the heat flow through the enclosures, means the system as a whole leads to substantial energy savings compared to SC1. The indoor air temperature T_i in summer is around 2–3 °C higher in SC3 than in SC1.

Furthermore, annual CO₂ emissions were quantified during the stage of home use, in accordance with Spain's current management of the electrical mix. It was also possible to make a first estimation of the environmental impacts deriving from the use of the air conditioning systems analysed in the study. The European Life Cycle Data Network (LCDN) database was used [73]. We considered that 0.41 kgCO₂, 0.00122 kgCH₄ and 0.0000465 kgN₂O are released to produce 1 kWh of electricity. The annual CO₂ emissions during the home's use stage could be evaluated by quantifying the simulations of annual final energy demand in the four scenarios SC1–SC4 set out in Table 6. The system's final energy demand and resulting CO₂ emissions were calculated using the factors provided by the Institute for Diversification and Energy Savings (IDAE by its Spanish acronym) [74], specifically: 2.21 MWh_p/MWh_f and 0.27 tCO₂eq/MWh. The reduction in annual CO₂ emissions resulting from these energy savings in the use phase was 4502.37 kg of CO₂ (Table 6). If we compare the wall and underfloor application of TCP panels, the annual CO₂ emissions in SC3 are 318.15 kg lower than in SC2, which represents a 5.15% reduction when TCP panels are used underfloor. These proven benefits of capillary tube mat radiant systems, such as TCP panels, combined with solar thermal energy production should be taken into account by public administrations. Pilot implementation support schemes or tax exemptions could be launched to reduce CO₂ emissions and other environmental impacts.

5.3. Incorporation of Solar Thermal Panels

The installation of solar thermal panels was dimensioned based on loads calculated using Design Builder. An annual energy demand for conditioning of 49.77 kWh/m²yr, with a heat pump using 40 kW in a cold regime in summer requires an installation of 24 m² of thermal solar panels on the roof. The market cost of the installation is EUR 10,889 (euros). According to previous estimates, these panels contribute 57.5% during energy demand peaks in summer, with maximum sunshine. In winter, it would be possible to achieve a value of 68.5%. The performance of an installation with 24 m² of solar thermal panels, at a 38° latitude and 45° inclination, is 71.4%. Given that the overall performance of the installation is 84.5%, the total power contribution to the TCP panel system is 4508 kWh/yr.

The results obtained by simulation with Design Builder were calibrated and corrected based on these solar energy results obtained in situ. They were contrasted with previous research on thermal energy in similar climates [75]. If we compare the two underfloor TCP panel scenarios SC3 and SC4, annual energy demand drops from 49.77 kWh/m²yr in SC3 to 28.30 kWh/m²yr in SC4, i.e., an energy saving of 43.14%. In winter, hot water is distributed to the capillary tube mats from the installation's accumulation tanks, while in summer, cold water is sent to the primary circuit distribution network at 7 °C–12 °C based on a lithium chloride solar cold system (LiCl), with chemical energy storage [76]. In cases of insufficient thermal leap, the water can be later cooled in the heat pump, until the set temperature of distribution to fan coil dehumidification is reached in the heat pump (7 °C). These results support the viability of these underfloor systems through TCP panels and a thermal solar panel system on the roof, with results similar to those obtained in previous research.

5.4. Breakdown of the Energy Consumption of the Various Installation Components

To determine the factors that contribute most to reducing the house's energy consumption, a disaggregated quantification of the energy consumption of each installation component was performed.

The energy consumption of the three systems analysed is disaggregated in Table 7, for all equipment, pumps, circulators, fans, fan coils, etc., and elements of the installations, as well as the solar panel energy contributions. The most significant reductions occur in the air-supply ventilators in SC1. When TCP panels function with water distribution, small circulation pumps are needed, not the ventilators. Their consumption amounts to 10.09 MWh/yr (4.82 + 5.27) in SC1, while in SC3 it is 3.066 MWh/yr (1.096 + 1.97). The equipment also requires greater power and energy consumption when operating with a greater thermal leap between the outdoor air temperature T_e and the indoor air temperature T_i , in addition to performing air dehumidification. The latter accounts for 13.83 MWh/yr in SC1 versus 10.02 MWh/yr in SC2 and 9.48 MWh/yr in SC3. These differences are partly offset by fan coil consumption in SC3 (4.81 MWh/yr), but the final balance is highly positive, presenting an energy saving of 25.19%.

Table 7. Calculation of annual energy consumption of each component in the installation. Comparison with convective systems.

Summer from 1 May to 30 November Winter from 1 December to 30 April Occupancy 5 People		SC1 All-Air	SC2 TCP Walls	SC3 TCP Floor	SC4 TCP Floor + Solar Panels	
1	Effective area	m ²	287.22	287.22	287.22	287.22
2	TCP ceramic panels Area	m ²		235	260	260
3	Maximum thermal load	W/m ²	80	75	70	70
4	Minimum flow of air renewal	m ³ /m ² h	1.70	1.70	1.70	1.70
5	Thermal leap of water in summer	k	6	3	3	3
6	System's run time	h/yr	5620	5620	5620	5620
	Cold pump run time	h/yr	2160	2160	2160	2160
	Total hours cooling is on	h/yr	744	260	246	246
	Total hours heating is on	h/yr	372	175	168	168
	Ventilation					
7	Air supply flow	m ³ /hm ²	18.32	2.45	2.45	2.45
8	Air supply volume	m ³ /h	2261	317	317	317
9	Ventilator power	kW	1.25	0.27	0.27	0.27
10	Power consumption	MWh/yr	4.82	1.096	1.096	1.096
	Cold pump					
11	Water flow	L/m ² h	10.70	21.5	20.1	20.1
12	Water volume	L/h	3073	6175	5972	5972
13	Power		0.10	0.25	0.24	0.24
14	Power consumption	MWh/año	0.45	0.88	0.82	0.82
	Ventilators and pumps					
15	Power consumption	MWh/yr	5.27	2.03	1.97	1.97
16	Comparison	%	100%	38.5%	37.4%	37.4%
	Fan coil dehumidifiers					
17	Power	kW		4.69	4.52	4.52
18	Power Consumption	MWh/yr		5.05	4.81	4.81
	Cooling system					
19	Emission power	W/m ²	85	72	70	70
20	Power	kW	18.47	14.21	13.77	13.77
21	Summer power consumption	MWh/yr	7.77	5.67	5.21	5.21
	Heating system					
22	Power	kW	16.8	15.87	15.49	15.49
23	Winter power consumption	MWh/yr	6.06	4.35	4.27	4.27
24	Solar energy supply					−6.67
	Circulators of water to the system					
25	Power					0.12
26	Power consumption					0.51
27	Annual energy consumption	MWh/yr	19.11	15.07	14.29	8.13
	Comparison	%	100%	78.87%	74.81%	42.54%

5.5. Investment Amortisation Approach

The last section of this comparative analysis focuses on the feasibility of implementing the TCP panel system and combining it with solar thermal panels in the real estate market. The costs of the energy consumed over those 30 years were based on the estimates of the simulations made with the Design Builder tool (Table 6), and an electrical mix cost of 0.142 EUR/kWh [77]. The investment costs in the 160 m² installation system of TCP panels, including the cost of the two substations and the three dehumidification fan coils, together amount to EUR 39,270. The installation cost of 24 m² of solar thermal panels was based—in accordance with the experience of companies in the sector—on a ratio of 453.7 EUR/m², including: labour costs, accumulation or inertia deposits, distribution equipment, circulation pumps and system management equipment. A total cost of EUR 10,889 was considered. Figure 10 and Table 8 show the results obtained for the whole investment's Global Cost in all 4 scenarios.



Figure 10. Global Cost Results over a 30-year period in the four scenarios under study.

Table 8. Global Cost Estimate according to UNE-EN 15459-1:2017.

	SC1 €/m ²	SC2 €/m ²	SC3 €/m ²	SC4 €/m ²
Investment cost	1320.2	1361.1	1351.7	1390.7
Indirect cost	53.6	61.3	64.0	71.8
Maintenance cost	107.1	90.4	91.5	123.8
Replacement cost	40.2	43.5	47.6	61.0
Energy cost	283.4	223.5	212.0	120.6
Global cost	1804.5	1779.8	1776.8	1767.9

The study's estimate of the amortisation of investments in air conditioning installations was based on the experience gained in previous studies [78]. The cost or investment in the 260 m² installation system of capillary mat TCP panels is between 38.69% (SC3) and 50.24% (SC2) higher than that of the conventional all-air system in SC1, and in the case of using solar thermal panels (SC4), up to 77.14% higher. We can estimate the amortisation periods of these investments according to the energy savings, maintenance costs, and possible flooring renovations, as shown in Table 9. The same applies to SC4 with the installation of solar panels and a solar cold production system using lithium chloride (LiCl). Although this investment leads to an increase in cost of 77.14% compared to SC1, and of 27.73% compared to SC3, the investment can be amortised within a reasonable period of time.

Table 9. Calculation of the investment amortisation period for scenarios SC2–SC4 versus SC1.

		SC1	SC2	SC3	SC4
All-air installation with heat pump	€	28,315			
Installation of TCP panels on the floor	€		42,541 €	39,270	50,159 €
Annual energy demand	kWh/año	19,110	15,078	14,290	8135
Annual savings	€		572.54	684.4	1558.45
Amortisation Period	años		24.85	16.01	14.01

As one can observe in the Global Cost results of the house in Figure 10, the differences per m² over the 30-year period is only 36.6 EUR/m²; that is, 2% versus 1804.5 EUR/m² in SC1. Furthermore, this shows the advantages of SC4, as the cost is 1767.9 EUR/m². We may conclude that despite higher upfront costs, the decision of applying TCP panel

systems combined with solar panels on the roof is ultimately cost-effective over a 30-year period. If we focus exclusively on radiant underfloor TCP panels (SC3), investments made compared to the all-air system (SC1) could a priori be amortised within 16 years, while the wall panel installation (SC2) would be amortised over 24 years, an excessively long period. If we compare the positioning of TCP panels underfloor (SC3) versus on the wall (SC2), we can conclude that radiant TCP floors are more cost-effective. The execution costs were reduced by EUR 3271, while the annual energy demand dropped by 5.15%. When incorporating solar thermal panels in both systems, the SC3 is more cost-effective. The investment would be amortised in 14 years, while the TCP wall would be amortised in 17.4 years.

When deciding whether to implement these systems in homes in Spain's Levante region, one should take into account the high comfort levels they procure, as well the significant reduction in CO₂ emissions and other environmental impacts they achieve, given the annual energy demand reductions of 25.19% (SC3) or 57.46% (SC4). These reductions in CO₂ emissions contribute to society's common good and should be supported by public administrations through financial incentives. User installations would thus become less expensive, and investment repayment periods would be shorter, between 8 and 10 years.

6. Conclusions

TCP ceramic panel underfloor conditioning systems bring high standards of comfort to single-family homes. They also lead to significant energy savings. It was possible to experiment and evaluate the thermal and energy behaviour of a detached house located near Albufereta beach in Alicante (Spain). Four scenarios were addressed based on different air conditioning systems as well as with and without the basement (SC1–SC4). Thermal and energy behaviours were compared. To validate the comparison, comfort parameters were adjusted in all scenarios, through the operating temperature T_o . The following results were obtained:

- TCP underfloor heating (SC3) systems were more energy efficient and more user-friendly than the current all-air system combined with winter hot water radiators (SC1). Annual energy demand was 25.19% lower.
- The radiant underfloor system with TCP panels (SC3), compared to the same panels positioned on the wall (SC2) is 5.15% more energy efficient. By reducing execution costs by EUR 3271 (almost 8%), the SC3 is more cost-effective. Investments would be amortised 3.4 years before the SC2.
- By installing 24 m² of solar thermal panels on the roof, with water accumulator tanks, an energy saving of 57.46% would be made with respect to the all-air system (SC1) and an energy saving of 43.14% compared to the installation of underfloor TCP panels (SC3). Investments in installation costs could be amortised in just over 14 years, with a reduction of 4502.37 kg of CO₂ emissions per year.
- The increase in investment for the installation of the capillary mat system using TCP panels could be amortised within a reasonable period of time compared to a conventional all-air installation (SC1). Regarding the house under study, the additional cost of EUR 10,955 would be amortised over 16 years, with an annual energy demand reduction of 4820 kWh/year and a consequent saving of EUR 684.4, with the current cost value in the electric mix of 0.142 EUR/kWh.

This study demonstrates the feasibility of using radiant surface conditioning systems in detached homes on the Mediterranean coast. These conditioning systems are healthier and more environmentally friendly, mainly when they are combined with solar thermal energy installations. A further step should be the parametric optimization of the radiant system by simulations.

Author Contributions: Article conceptualization, V.E.-I.; methodology, investigation, validation, resources, and writing, N.H.W., A.S.-O., and V.E.-I.; software, A.S.-O. and V.E.-I.; project administration

and funding acquisition, V.E.-I. All authors have read and agreed to the published version of the manuscript.

Funding: This research has been funded by the projects “Generation of knowledge on the multisensory interaction of human beings with the environments for the development of new products and services in the ceramics sector (4SENSES)” (ACOMP/2010/040). Complementary aid for R + D + i projects. Generalitat Valenciana. Ministry of Education. Spain, 2010; and “Research on sustainable architectural and bioclimatic conditioning solutions using ceramic materials (ASCER1-18I)”. Spanish Association of Manufacturers of Ceramic Tiles and Flooring (ASCER). 2017–2018.

Institutional Review Board Statement: Not applicable.

Informed Consent Statement: Not applicable.

Data Availability Statement: The monitoring data contained in the article are not available for reasons of confidentiality. The data presented in this study, derived from the Design Builder tool, are available upon request from the corresponding author.

Acknowledgments: Our thanks to Almudena Espinosa for his help in monitorization of the house; to José Luis Sanjuan for the Design Builder simulations; and to Francisco José Aldea and Ginés Gómez for their help with the TCP panel mounting.

Conflicts of Interest: The funders had no role in the design of the study; in the collection, analyses, or interpretation of data; in the writing of the manuscript, or in the decision to publish the results.

References

- Karmann, C.; Schiavon, S.; Bauman, F. Thermal comfort in buildings using radiant vs. all-air systems: A critical literature review. *Build. Environ.* **2017**, *111*, 123–131. [\[CrossRef\]](#)
- Cacabelos, C.; Eguía, P.; Míguez, J.L.; Granada, E.; Arce, M.E. Calibrated simulation of a public library HVAC system with a ground-source heat pump and a radiant floor using TRNSYS and GenOpt. *Energy Build.* **2015**, *108*, 114–126. [\[CrossRef\]](#)
- Feng, J.; Schiavon, S.; Bauman, F. Cooling load differences between radiant and air systems. *Energy Build.* **2013**, *65*, 310–321. [\[CrossRef\]](#)
- Acikgoz, O.; Karakoyun, Y.; Yumurtaci, Z.; Dukhan, N.; Dalkılıç, A.S. Realistic experimental heat transfer characteristics of radiant floor heating using sidewalls as heat sinks. *Energy Build.* **2019**, *183*, 515–526. [\[CrossRef\]](#)
- Wang, D.; Lu, L.; Cui, P. A new analytical solution for horizontal geothermal heat exchangers with vertical spiral coils. *Int. J. Heat Mass Transf.* **2016**, *100*, 111–120. [\[CrossRef\]](#)
- Kim, M.J.; Lee, S.-R.; Yoon, S.; Jeon, J.-S. An applicable design method for horizontal spiral-coil-type ground heat exchangers. *Geothermics* **2018**, *72*, 338–347. [\[CrossRef\]](#)
- Echarri-Iribarren, V. Conditioning using ceramic floor panels with capillary tube mats and solar thermal panels on the Mediterranean coast: Energy savings and investment amortization. *Energy Build.* **2019**, *202*, 109334. [\[CrossRef\]](#)
- Zhang, C.; Pomianowski, M.; Heiselberg, P.K.; Yu, T. A review of integrated radiant heating/cooling with ventilation systems—Thermal comfort and indoor air quality. *Energy Build.* **2020**, *223*, 110094. [\[CrossRef\]](#)
- Obrecht, T.P.; Kunič, R.; Jordan, S.; Dovjak, M. Comparison of Health and Well-Being Aspects in Building Certification Schemes. *Sustainability* **2019**, *11*, 2616. [\[CrossRef\]](#)
- Rhee, K.-N.; Olesen, B.W.; Kim, K.W. Ten questions about radiant heating and cooling systems. *Build. Environ.* **2017**, *112*, 367–381. [\[CrossRef\]](#)
- Lin, B.; Wang, Z.; Sun, H.; Zhu, Y.; Ouyang, Q. Evaluation and comparison of thermal comfort of convective and radiant heating terminals in office buildings. *Build. Environ.* **2016**, *106*, 91–102. [\[CrossRef\]](#)
- Mustakallio, P.; Bolashikov, Z.D.; Rezgals, L.; Lipczynska, A.; Melikov, A.K.; Kosonen, R. Thermal environment in a simulated double office room with convective and radiant cooling systems. *Build. Environ.* **2017**, *123*, 88–100. [\[CrossRef\]](#)
- Krzaczek, M.; Florczuk, J.; Tejchman, J. Improved energy management technique in pipe-embedded wall heating/cooling system in residential buildings. *Appl. Energy* **2019**, *254*, 113711. [\[CrossRef\]](#)
- Catalina, T.; Virgone, J.; Kuznik, F. Evaluation of thermal comfort using combined CFD and experimentation study in a test room equipped with a cooling ceiling. *Build. Environ.* **2009**, *44*, 1740–1750. [\[CrossRef\]](#)
- Sun, H.; Wu, Y.; Lin, B.; Duan, M.; Lin, Z.; Li, H. Experimental investigation on the thermal performance of a novel radiant heating and cooling terminal integrated with a flat heat pipe. *Energy Build.* **2020**, *208*, 109646. [\[CrossRef\]](#)
- Yeom, G.; Jung, D.E.; Do, S.L. Improving a Heating Supply Water Temperature Control for Radiant Floor Heating Systems in Korean High-Rise Residential Buildings. *Sustainability* **2019**, *11*, 3926. [\[CrossRef\]](#)
- Márquez, A.A.; López, J.M.C.; Hernández, F.F.; Muñoz, F.D.; Andres, A.C. A comparison of heating terminal units: Fan-coil versus radiant floor, and the combination of both. *Energy Build.* **2017**, *138*, 621–629. [\[CrossRef\]](#)
- Seo, J.-M.; Song, D.; Lee, K.H. Possibility of coupling outdoor air cooling and radiant floor cooling under hot and humid climate conditions. *Energy Build.* **2014**, *81*, 219–226. [\[CrossRef\]](#)

19. Hernández, F.F.; López, J.M.C.; Fernández-Gutiérrez, A.; Muñoz, F.D.; Fernandez, F. A new terminal unit combining a radiant floor with an underfloor air system: Experimentation and numerical model. *Energy Build.* **2016**, *133*, 70–78. [CrossRef]
20. Ansuini, R.; Larghetti, R.; Giretti, A.; Lemma, M. Radiant floors integrated with PCM for indoor temperature control. *Energy Build.* **2011**, *43*, 3019–3026. [CrossRef]
21. Sun, W.; Zhang, Y.; Ling, Z.; Fang, X.; Zhang, Z. Experimental investigation on the thermal performance of double-layer PCM radiant floor system containing two types of inorganic composite PCMs. *Energy Build.* **2020**, *211*, 109806. [CrossRef]
22. Zhou, Y.; Zheng, S.; Zhang, G. A review on cooling performance enhancement for phase change materials integrated systems—flexible design and smart control with machine learning applications. *Build. Environ.* **2020**, *174*, 106786. [CrossRef]
23. Movinord Climatización. Manual de Climatización Tranquila. Available online: <http://www.movinord.com/descargas/Climatizacion%202008.pdf> (accessed on 11 March 2019).
24. Mikeska, T.; Svendsen, S. Dynamic behavior of radiant cooling system based on capillary tubes in walls made of high performance concrete. *Energy Build.* **2015**, *108*, 92–100. [CrossRef]
25. Zhou, G.; He, J. Thermal performance of a radiant floor heating system with different heat storage materials and heating pipes. *Appl. Energy* **2015**, *138*, 648–660. [CrossRef]
26. ISO. ISO-11855: 2012, *Building Environment Design—Design, Dimensioning, Installation and Control of Embedded Radiant Heating and Cooling Systems*; International Organization for Standardization: Geneva, Switzerland, 2012.
27. Tang, H.; Zhang, T.; Liu, X.; Li, C. A novel approximate harmonic method for the dynamic cooling capacity prediction of radiant slab floors with time variable solar radiation. *Energy Build.* **2020**, *223*, 110117. [CrossRef]
28. Feng, J.; Schiavon, S.; Bauman, F. New method for the design of radiant floor cooling systems with solar radiation. *Energy Build.* **2016**, *125*, 9–18. [CrossRef]
29. De Dear, R.J.; Akimoto, T.; Arens, E.A.; Brager, G.; Candido, C.; Cheong, K.W.D.; Li, B.; Nishihara, N.; Sekhar, S.C.; Tanabe, S.; et al. Progress in thermal comfort research over the last twenty years. *Indoor Air* **2013**, *23*, 442–461. [CrossRef]
30. Beka. *Capillary Tube Systems. Product Data Sheets. Technical Information G0*; Beka Heiz-und Kühlmatten: Berlin, Germany, 2008. Available online: <https://www.beka-klima.de/en/heating-cooling/capillary-tube-technology/> (accessed on 5 March 2019).
31. Zhao, M.; Gu, Z.; Kang, W.; Liu, X.; Zhang, L.Y.; Jin, L.; Zhang, Q. Experimental investigation and feasibility analysis on a capillary radiant heating system based on solar and air source heat pump dual heat source. *Appl. Energy* **2017**, *185*, 2094–2105. [CrossRef]
32. Climate WellTM 10. Design Guidelines. Available online: http://www.solarcombiplus.eu/docs/SolarCombi_ClimateWell_trainingmaterial5.pdf (accessed on 12 March 2019).
33. Patel, J.; Pandya, B.; Mudgal, A. Exergy Based Analysis of LiCl-H₂O Absorption Cooling System. *Energy Procedia* **2017**, *109*, 261–269. [CrossRef]
34. Widiatmojo, A.; Gaurav, S.; Ishihara, T.; Yasukawa, K.; Uchida, Y.; Yoshioka, M.; Tomigashi, A. Using a capillary mat as a shallow heat exchanger for a ground source heat pump system. *Energy Build.* **2020**, *209*, 109684. [CrossRef]
35. Zamora, M. Proyecto Geocool: Empleo de Bombas de Calor Acopladas A Intercambiadores Geotérmicos. Available online: http://blog.energesis.es/wp-content/uploads/2008_03_ENERGETICA_XXI.pdf (accessed on 9 March 2019).
36. Yeom, D.; La Roche, P. Investigation on the cooling performance of a green roof with a radiant cooling system. *Energy Build.* **2017**, *149*, 26–37. [CrossRef]
37. Haiwen, S.; Lin, D.; Xiangli, L.; Yingxin, Z. Quasi-dynamic energy-saving judgment of electric-driven seawater source heat pump district heating system over boiler house district heating system. *Energy Build.* **2010**, *42*, 2424–2430. [CrossRef]
38. Li, Z.; Songtao, H. Research on the heat pump system using seawater as heat source or sink. *Build. Energy Environ.* **2006**, *25*, 34–38.
39. Tian, Z.; Yin, X.; Ding, Y.; Zhang, C. Research on the actual cooling performance of ceiling radiant panel. *Energy Build.* **2012**, *47*, 636–642. [CrossRef]
40. Zhao, R.; Tuan, C.Y.; Luo, B.; Xu, A. Radiant heating utilizing conductive concrete tiles. *Build. Environ.* **2019**, *148*, 82–95. [CrossRef]
41. Mikeska, T.; Fan, J.; Svendsen, S. Full scale measurements and CFD investigations of a wall radiant cooling system integrated in thin concrete walls. *Energy Build.* **2017**, *139*, 242–253. [CrossRef]
42. Choi, N.; Yamanaka, T.; Sagara, K.; Momoi, Y.; Suzuki, T. Displacement ventilation with radiant panel for hospital wards: Measurement and prediction of the temperature and contaminant concentration profiles. *Build. Environ.* **2019**, *160*, 106197. [CrossRef]
43. Rucevskis, S.; Akishin, P.; Korjakins, A. Parametric analysis and design optimisation of PCM thermal energy storage system for space cooling of buildings. *Energy Build.* **2020**, *224*, 110288. [CrossRef]
44. Ning, B.; Chen, Y.; Liu, H.; Zhang, S. Cooling capacity improvement for a radiant ceiling panel with uniform surface temperature distribution. *Build. Environ.* **2016**, *102*, 64–72. [CrossRef]
45. Cantavella, V.; Bannier, E.; Silva, G.; Muñoz, S.; Portolés, J.; Algora, E.; Garcia, M.A. Dynamics of thermal performance of an electric radiant floor with removable ceramic tiles. In Proceedings of the 2010 11th World Congress on Ceramic Tile Quality, Castellon, Spain, 15–16 February 2010.
46. Koschenz, M.; Lehmann, B. Development of a thermally activated ceiling panel with PCM for application in lightweight and retrofitted buildings. *Energy Build.* **2004**, *36*, 567–578. [CrossRef]

47. Echarri Iribarren, V.; Galiano Garrigós, A.L.; González Avilés, A.B. Ceramics and healthy heating and cooling systems: Thermal ceramic panels in buildings. Conditions of comfort and energy demand versus convective systems. *Inf. Construcción* **2016**, *68*, 19–32.
48. Echarri, V.; Oviedo, E.; Lázaro, V. Panel de Acondicionamiento Térmico Cerámico. Patent P201001626 28 December 2010. INVENES, OEPM –Oficina Española de Patentes y Marcas. Available online: <http://invenes.oepm.es/InvenesWeb/detalle?referencia=P201001626> (accessed on 10 March 2019).
49. Echarri-Iribarren, V. Thermal Ceramic Panels and Passive Systems in Mediterranean Housing: Energy Savings and Environmental Impacts. *Sustainability* **2017**, *9*, 1613. [CrossRef]
50. Kottek, M.; Grieser, J.; Beck, C.; Rudolf, B.; Rubel, F. World Map of the Köppen-Geiger climate classification updated. *Meteorol. Z.* **2006**, *15*, 259–263. [CrossRef]
51. Kottek, M.; Grieser, J.; Beck, C.; Rudolf, B.; Rubel, F. *World Map of the Köppen-Geiger Climate Classification Updated. High Resolution Map and Data (Version March 2017)*; KMZ File for Google Earth (high res): Global_1986-2010_KG_5m.kmz; Climate Change & Infectious Diseases: Wien, Austria, 2017. Available online: <http://koeppen-geiger.vu-wien.ac.at> (accessed on 13 April 2019).
52. Orden FOM/1635/2013, de 10 de Septiembre, por la que se Actualiza el Documento Básico DB-HE Ahorro de Energía, del Código Técnico de la Edificación, Aprobado por Real Decreto 314/2006, de 17 de marzo; (Publicado en: <BOE> núm. 219, de 12 de Septiembre de 2013, Páginas 67137–67209); Spanish Ministry of Public Works and Transport: Madrid, Spain, 2013. Available online: <https://www.codigotecnico.org/index.php/menu-ahorro-energia.html> (accessed on 16 April 2019).
53. Bojić, M.; Cvetković, D.; Miletić, M.; Malešević, J.; Boyer, H. Energy, cost, and CO2 emission comparison between radiant wall panel systems and radiator systems. *Energy Build.* **2012**, *54*, 496–502. [CrossRef]
54. International Organization for Standardization. ISO 9972:2015 Thermal Performance of Buildings—Determination of Air Permeability of Buildings—Fan Pressurization Method. (ISO 9972:1996, Modified). 2002. Available online: <https://www.iso.org/standard/55718.html> (accessed on 9 March 2019).
55. 2017 ASHRAE Handbook—Fundamentals; American Society of Heating, Refrigeration and Air Conditioning Engineers: Atlanta, GA, USA, 2017; ISBN 9781939200587. Available online: <https://www.ashrae.org/technical-resources/ashrae-handbook/description-2017-ashrae-handbook-fundamentals> (accessed on 20 March 2019).
56. UNE EN ISO 10456:2012. Materiales y Productos Para la Edificación. Propiedades Higrotérmicas. Valores Tabulados de Diseño y Procedimientos Para la Determinación de los Valores Térmicos Declarados. 2012. Available online: <http://www.aenor.es/aenor/normas/normas/fichanorma.asp?tipo=N&codigo=N0049362#.Wgbq4tThCmw> (accessed on 9 October 2017).
57. Feijó-Muñoz, J.; Pardal, C.; Echarri-Iribarren, V.; Fernández-Agüera, J.; De Larriva, R.A.; Calderín, M.M.; Poza-Casado, I.; Padilla-Marcos, M.Á.; Meiss, A. Energy impact of the air infiltration in residential buildings in the Mediterranean area of Spain and the Canary islands. *Energy Build.* **2019**, *188–189*, 226–238. [CrossRef]
58. Andújar Márquez, J.M.; Martínez Bohórquez, M.Á.; Gómez Melgar, S. A New Metre for Cheap, Quick, Reliable and Simple Thermal Transmittance (U-Value) Measurements in Buildings. *Sensors* **2017**, *17*, 2017. [CrossRef]
59. Nardi, I.; Ambrosini, D.; De Rubeis, T.; Sfarra, S.; Perilli, S.; Pasqualoni, G. A comparison between thermographic and flow-meter methods for the evaluation of thermal transmittance of different wall constructions. *J. Phys. Conf. Ser.* **2015**, *655*, 012007. [CrossRef]
60. *Thermal Insulation. Building Elements. In-Situ Measurement of Thermal Resistance and Thermal Transmittance. Part 1: Heat Flow Metre Method*; ISO 9869-1:2014; International Organization for Standardization: Geneva, Switzerland, 2014. Available online: <https://www.iso.org/standard/59697.html> (accessed on 15 March 2019).
61. Balghouthi, M.; Chahbani, M.; Guizani, A. Investigation of a solar cooling installation in Tunisia. *Appl. Energy* **2012**, *98*, 138–148. [CrossRef]
62. Sarbu, I.; Sebarchievici, C. Review of solar refrigeration and cooling systems. *Energy Build.* **2013**, *67*, 286–297. [CrossRef]
63. Bataineh, K.; Taamneh, Y. Review and recent improvements of solar sorption cooling systems. *Energy Build.* **2016**, *128*, 22–37. [CrossRef]
64. Sancho Ávila, J.M.; Riesco Martín, J.; Jiménez Alonso, C.; Sánchez de Cos, M.D.; Montero Cadalso, J.; López Bartolomé, M. *Atlas de Radiación Solar en España Utilizando Datos del SAF de Clima de Eumetsat*; AEMET: Madrid, Spain, 2005. Available online: http://www.aemet.es/documentos/es/serviciosclimaticos/datosclimatologicos/atlas_radiacion_solar/atlas_de_radiacion_24042012.pdf (accessed on 10 March 2019).
65. González-Roubaud, E.; Pérez-Osorio, D.; Prieto, C. Review of commercial thermal energy storage in concentrated solar power plants: Steam vs. molten salts. *Renew. Sustain. Energy Rev.* **2017**, *80*, 133–148. [CrossRef]
66. Li, H.; Bi, Y.; Qin, L.; Zang, G. Absorption solar-ground source heat pump: Life cycle environmental profile and comparisons. *Geothermics* **2020**, *87*, 101850. [CrossRef]
67. *Energy Performance of Buildings—Economic Evaluation Procedure for Energy Systems in Buildings—Part 1: Calculation Procedures*; UNE-EN 15459-1:2017; Module M1-14; European Committee for Standardization (CEN): Brussels, Belgium, 2017. Available online: https://standards.cen.eu/dyn/www/?p=204:110:0:::FSP_PROJECT,FSP_ORG_ID:40932,6209&cs=110690DD8F9BE238B61D722D035C11CAE (accessed on 11 June 2019).
68. Theodosiou, T.G.; Tsikaloudaki, A.G.; Kontoleon, K.J.; Bikas, D.K. Thermal bridging analysis on cladding systems for building facades. *Energy Build.* **2015**, *109*, 377–384. [CrossRef]
69. Bienvenido-Huertas, D.; Moyano, J.; Marin, D.; Fresco-Contreras, R. Review of in situ methods for assessing the thermal transmittance of walls. *Renew. Sustain. Energy Rev.* **2019**, *102*, 356–371. [CrossRef]

70. Herramienta Unificada Lider-Calener (HULC). *Orden FOM/1635/2013, de 10 de Septiembre (BOE de 12 de septiembre), por la que se Actualiza el Documento Básico DB HE «Ahorro de Energía», del CTE*; Ministerio de Ciencia e Innovación: Madrid, Spain, 2013. Available online: <https://www.codigotecnico.org/index.php/menu-recursos/menu-aplicaciones/282-herramientaunificada-lider-calener.html> (accessed on 9 March 2019).
71. Domínguez-Muñoz, F.; Cejudo-López, J.M.; Carrillo-Andrés, A. Uncertainty in peak cooling load calculations. *Energy Build.* **2010**, *42*, 1010–1018. [[CrossRef](#)]
72. Stetiu, C. Energy and peak power savings potential of radiant cooling systems in US commercial buildings. *Energy Build.* **1999**, *30*, 127–138. [[CrossRef](#)]
73. European Commission. LCDN—The Life Cycle Data Network. Available online: <https://eplca.jrc.ec.europa.eu/LCDN/> (accessed on 9 March 2019).
74. Instituto para la Diversificación y Ahorro de Energía (IDAE). *Informe de Balance de Consumo de Energía Final. 1990–2018*; Instituto para la Diversificación y Ahorro de Energía: Madrid, Spain, 2018. Available online: <http://sieeweb.idae.es/consumofinal/> (accessed on 30 October 2020).
75. Corona, B.; de la Rúa, C.; San Miguel, G. Socio-economic and environmental effects of concentrated solar power in Spain: A multiregional input output analysis. *Sol. Energy Mater. Sol. Cells* **2016**, *156*, 112–121. [[CrossRef](#)]
76. Wang, R.Z.; Xia, Z.Z.; Wang, L.W.; Lu, Z.S.; Li, S.L.; Li, T.X.; Wu, J.Y.; He, S. Heat transfer design in adsorption refrigeration systems for efficient use of low-grade thermal energy. *Energy* **2011**, *36*, 5425–5439. [[CrossRef](#)]
77. IDAE. Informe de Precios Energéticos Regulados. 2017. Available online: http://www.idae.es/sites/default/files/estudios_informes_y_estadisticas/tarifas_reguladas_julio_2017.pdf (accessed on 7 March 2019).
78. Al Ajmi, A.; Abou-Ziyan, H.; Ghoneim, A. Achieving annual and monthly net-zero energy of existing building in hot climate. *Appl. Energy* **2016**, *165*, 511–521. [[CrossRef](#)]